Wood as Polar Size Exclusion Chromatography Media: Implications to Adhesive Performance*

Christopher Hunt Jane O'Dell Joseph Jakes
Warren J. Grigsby Charles R. Frihart

Abstract

Although it is well known that wood can absorb liquids, the full impact of this phenomenon on resulting adhesive cure and performance is not well understood. In a related soy adhesive study, aspects of this phenomenon were not fully anticipated and resulted in a significant impact on adhesive bond quality. In essence, the wood being bonded acted like chromatography media, filtering relatively smaller molecules from the surrounding adhesive matrix and altering the local composition of the adhesive material. Through the use of soy adhesives containing glycerin, the infiltration of glycerin analogs into wood cell walls has been determined and related with the impact on bondline and wood properties. The impacts of infiltration and chromatographic separation on the cured adhesive are also discussed.

Water not only flows into wood cell lumens, but also infiltrates into the cell walls, causing them to swell. Other polar chemicals can also infiltrate cell walls, but as the molecular weight increases (Tarkow et al. 1965) or the hydrogen bonding capacity of the chemical decreases (Mantanis et al. 1994, Obataya and Gril 2005), both absorption and swelling decrease. Although the intentional infiltration of chemicals into cell walls has long been studied, the transfer of specific components from adhesives into cell walls has not been widely appreciated. Low-molecular-weight (LMW) adhesive components often cause adhesion problems through formation of a weak interphase layer (Bikerman 1967) or adhesive cohesion problems by plasticization of the adhesive. However, after a liquid adhesive is applied to wood, some components can move from the bulk adhesive into the cell wall by infiltration (Kamke and Lee 2007; Konnerth et al. 2008; Grigsby and Thumm 2010, 2012). In this respect the wood can be considered to be acting similarly to a polar size exclusion chromatography column, removing small polar molecules from the liquid adhesive. This separation of adhesive components can have a large impact on the wood that absorbs these materials, the adhesive left behind in the glueline, and accordingly, the bond performance.

Infiltration is used here to mean the movement of small molecules from the adhesive into the wood cell wall. Many use the term penetration for this, but the general term penetration involves two very distinct phenomena, flow and infiltration, governed by very different criteria (Frihart 2006). Flow is the bulk movement of adhesive through empty spaces, influenced by viscosity, surface energies, and fluid dynamics. In contrast, infiltration is the molecular mixing of adhesive components with the cell wall polymers, governed by the molecular sizes of adhesive components, swelling state of the cell wall, and the solubility parameters of both. Moreover, only defining molecular size is insufficient: small molecules with relatively poor hydrogen bonding capacity such as toluene will not infiltrate wood

The authors are, respectively, Research Chemist, Physical Science Technician, and Research Materials Engineer, USDA Forest Serv., Forest Products Lab., Madison, Wisconsin (cghunt@fs.fed.us [corresponding author], janeodell@fs.fed.us, jjakes@fs.fed.us); Research Leader, SCION, Rotorua, New Zealand (Warren.Grigsby@scionresearch.com); and Team Leader, Wood Adhesives, Performance Enhanced Biopolymers, USDA Forest Serv., Forest Products Lab., Madison, Wisconsin (cfrihart@fs.fed.us). This paper was received for publication in April 2014. Article no. 14-00039.

* This article is part of a series of 10 selected articles addressing a theme of efficient use of wood resources in wood adhesive bonding research. The research reported in these articles was presented at the International Conference on Wood Adhesives, held on October 9–11, 2013, in Toronto, Canada. All 10 articles are published in this issue of the *Forest Products Journal* (Vol. 65, No. 1/2).

©Forest Products Society 2015.

Forest Prod. J. 65(1/2):9–14.
doi:10.13073/FPJ-D-14-00039

nearly as well as similarly sized molecules with good hydrogen bonding such as pyridine (Mantanis et al. 1994).

The migration of LMW adhesive components from in situ polymerized adhesives such as phenol-formaldehyde resins, resorcinol-formaldehyde resins, urea-formaldehyde (UF), and melamine-(urea-)formaldehyde into the cell wall, and the subsequent reinforcement of the cell wall, have been discussed by Frihart (2009). The infiltration and hardening of adhesive oligomers in the cell wall is proposed to both repair damage to cells near the bond surface and modify the cell wall; this results in a more gradual gradient of material properties between the bondline and the bulk wood, resulting in less concentration of swelling stresses when wet and therefore better bond performance. Multiple nanoindentation studies (Gindl and Gupta 2002; Gindl et al. 2004a, 2004b; Konnerth and Gindl 2006; Konnerth et al. 2007; Hunt et al. 2010; Liang et al. 2011; Stöckel et al. 2012) have shown a hardening or stiffening of cell walls adjacent to bondlines with in situ polymerized adhesives. Pre-polymerized adhesives, such as polyurethane and poly(vinyl acetate), by contrast, are too large to enter the cell wall and have not shown this effect (Gindl et al, 2004a, 2004b; Konnerth et al. 2007).

While wood modification is commonly observed, modification of the adhesive because it is cured in the presence of wood is much more subtle and not universally observed (Konnerth et al. 2006), Associated work, also presented at this conference (Grigsby et al. 2015) demonstrated a dramatic difference in the extractability of UF resin components when cured neat versus on wood. Curing adhesive neat yielded almost no cold water extractables while approximately 50 percent of the nitrogen due to the urea component was extractable from the UF-bonded fiberboard, suggesting that at least a portion of the UF resin within the board does not become part of a large, cross-linked network. Furthermore, lower UF resin loading resulted in higher extractability, consistent with the idea that UF oligomers infiltrate the cell wall, but are so dilute they do not fully polymerize. In this case, the interaction with wood has clearly changed the properties of the final adhesive.

Another recent report (Frazier 2013) discussed structure and property differences between neat polyurethane adhesive and excised bondlines of the same material. Some believe that extractives sometimes migrate into polyurethane adhesive and interfere with curing (anonymous conference attendee, 2013).

Dramatic examples of the impact of infiltration on cured adhesive properties are observable in soy adhesive formulations containing glycerin. Some soy-glycerin plywood adhesives, with up to three parts glycerin to one part soy flour, bond wood well but have little stiffness or cohesive strength when cured neat. In contrast, soy flour alone when mixed with water and dried makes a very stiff material. We hypothesized that LMW materials such as glycerin migrate into the wood, leaving adhesive in the glueline with a low glycerin content, and therefore properties more similar to pure soy than the applied soy-glycerin mixture. This would imply that the cells adjacent to the bondline contain glycerin, a wood plasticizer (Yan et al. 2011). In this article, experiments are presented that test whether glycerin migrates from the adhesive into wood cells, and the implications to wood adhesives in general are discussed. In this study, the glycerin added to soy adhesives was replaced with chlorinated analogs to aid analyses. Nanoindentation was used to determine elastic modulus and hardness of the cell walls adjacent to the bondline, with complementary scanning electron microscopy–energy dispersive spectroscopy (SEM-EDS) used to measure concentration of the chlorinated glycerin analogs in these same cells. This enabled observation of any correlation between the movement of glycerin analogs from adhesive into cell walls and any resulting changes in cell wall mechanical properties. Supporting experiments on thermal softening of soy adhesives suggest the LMW components inherent in soy flour have similar behavior.

Materials and Methods

Soy adhesive was 21 percent (wt/wt) soy flour (100 mesh, 90 PDI, Prolia 100/90, Cargill Inc., Cedar Rapids, Iowa), 21 percent (wt/wt) glycerin analog (3-chloro-1,2 propanediol or 3-chloro-1-propanol; Sigma-Aldrich, St. Louis, Missouri), and 58 percent (wt/wt) reverse osmosis (RO) water. The water and analog were mixed for 30 seconds in an IKA Turrax homogenizer. Soy flour was then added in three parts with stirring after each addition and then mixed 2 minutes, scraping the sides of the container two times. The adhesive was left to rest 60 minutes before bonding.

Neat soy adhesives on the left side in Figure 1 were the same soy as above, with the exception that just RO water

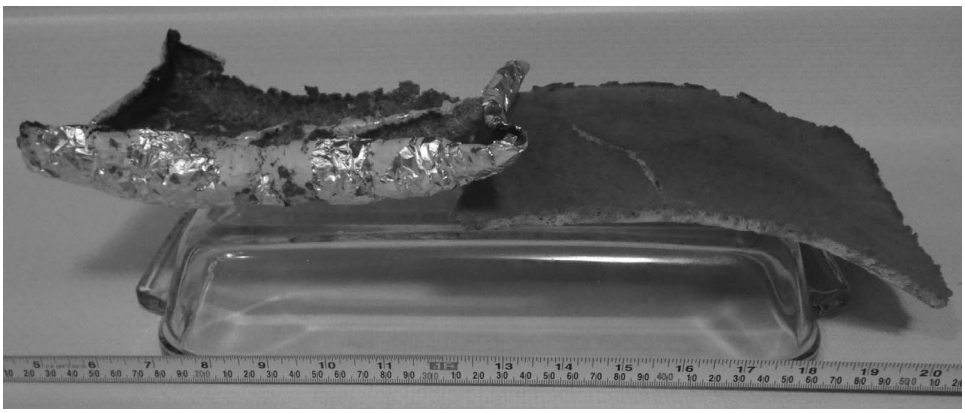

Figure 1.—Dried soy flour–polyamidoamine epichlorohydrin. Mixed with water and dried (left) and mixed with water and glycerin and then dried (right).

Table 1.—Hansen's solubility parameters of glycerin, glycerin analogs used in this study, lignin, and cellulose.

Compound	Hansen's solubility parameters (δ/MPa$^{0.5}$)			
	Total	Dispersion	Polar	H bond
Glycerin (Hansen 2000)	36.1	17.4	12.1	29.3
3 Chloro 1,2 propanediol (est)[a]	28.8	18.3	8.3	20.6
3 Chloro 1 propanol (Hansen 2000)	23.6	17.5	5.7	14.7
"Lignin" (Hansen and Bjorkman 1998)	~29	~22	~14	~14
"Cellulose" (Hansen and Bjorkman 1998)	~29	~17	~17	~16

[a] est = estimated based on difference between nonchlorinated 1-propanol and 1,2-propanediol.

was used instead of water-glycerin analog; additionally PAE (polyamidoamine epichlorohydrin; Ashland Water Technologies 1920A), a wet strength agent, was added because it is used in many commercial formulations, although PAE does not affect the look or stiffness of the adhesive when dry. The adhesive on the right of Figure 1 also contains glycerin.

Loblolly pine specimens (*Pinus taeda*) were cut to 2.5 mm (radial) by 5 mm (tangential) by 5 mm (longitudinal), with bonding faces surfaced with a sled microtome. A small amount of prepared adhesive was spread over the tangential face of one wood sample and then a second wood sample was placed on top. The specimen was pressed in a TA Q800 dynamic mechanical analyser (DMA) in the penetration fixture. The supplied top probe was replaced with a flat 12.5-mm-diameter disc; 17 N (0.68MPa) load was applied. The system was equilibrated at 35°C, ramp at 20°C/min to 120°C, held 5 minutes, and ballistic (air) cooled. The samples were conditioned 1 week at 21°C, 50 percent relative humidity before testing.

Nanoindentation was performed with a Hysitron (Minneapolis, Minnesota) TriboIndenter equipped with a diamond Berkovich probe. High-quality transverse surfaces of the bondline were prepared for nanoindentation with a diamond knife fit in an ultramicrotome (Jakes et al. 2008, 2009). Load-control multiload nanoindents were used. They consisted of nine load–hold–unload–hold at partial unload cycles, with each cycle with a progressively higher load up to 0.5 mN in the final cycle. The machine compliance and probe area function were calibrated from a series of nanoindents in a fused silica standard following standard protocols (Oliver and Pharr 1992, Stone et al. 2010). The structural compliance method was used to account for edge effects and specimen-scale flexing. After correcting the nanoindent load-depth trace for structural compliance, the elastic modulus and hardness were assessed from all nine unloading segments following the Oliver-Pharr method (Oliver and Pharr 1992) assuming a cell wall Poisson's ratio of 0.45 (Wimmer et al. 1997). We found unloading segments with a contact area of less than 0.09 μm^2, typically only in the first cycle, that were affected by tip roundness for the Berkovich probe used and we excluded these nanoindents from the analyses. Nanoindents were placed on the tangential side in the S2 cell wall lamina within rows of daughter cells that extended from the bondline into the wood adherend. The cells within a daughter cell row far from the bondline can be used as a control for the cells within the row near the bondline.

SEM-EDS was used to estimate chlorine, and therefore chloropropanol and chloropropanediol content, inside the cell walls adjacent to the bondline. SEM-EDS point scans were taken with the LEO EVO 40 at a variable pressure of 52 Pa at 1.2 nA and 15 kV at the center of the cell walls in the rows of cells tested with nanoindentation. EDS analysis was performed using an IXRF 550i system with a 50-mm SDD detector (IXRF Systems, Inc., Houston, Texas). Spectra were collected for 100 seconds at each point.

Results and Discussion

Figure 1 shows the image of two neat soy-PAE adhesives after drying in the oven. On the left is 21 percent soy–2 percent PAE (wet strength agent)–77 percent water and on the right is 21 percent soy–2 percent PAE–21 percent glycerin–56 percent water. Without glycerin, the adhesive dries hard and stiff, making a crisp sound when tapped with a fingernail. On the right, the softness of the glycerin-soy is evident by the way it sags when unsupported. The neat glycerin containing adhesive also had low cohesive strength and it tears easily.

The 3 chloro-1,2 propanediol (diol) and 3 chloro-1-propanol (mono-ol) were chosen as substitutes for glycerin because they could be traced using SEM-EDS. Their solubility parameters (Table 1) and structures (Fig. 2) are compared with glycerin and wood components. Lignin and cellulose are in quotation marks because of the inherent uncertainty in solubility parameters for these materials.

Figure 3 shows the elastic modulus and hardness obtained by nanoindents in cells adjacent to the bondline. With regard to elastic modulus, the diol-infiltrated wood (open symbols) appears to have a trend toward lower elastic modulus nearer the bondline, as would be expected if glycerin analogs had infiltrated the cells near the bondline and plasticized the cell walls. With regard to hardness, the trend for diol-infiltrated cells is less conclusive. For one row of daughter cells, the hardness decreases near the bondline, consistent with the trend in elastic modulus, but in the other row, there is no trend with distance from the bondline. The trend for mono-ol–infiltrated cells in elastic modulus and hardness is almost flat, and there is not a clear relationship between these properties and distance from the bondline.

To investigate if trends in cell wall mechanical properties were related to cell wall infiltration of diol or mono-ol, SEM-EDS measurements of the same cell walls were obtained (Fig. 4) to estimate the concentration of glycerin analog. Although EDS data are not quantitative and the

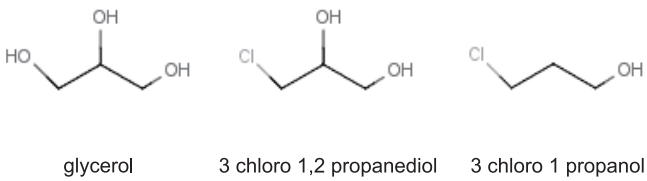

Figure 2.—Structures of glycerin and chlorinated compounds used as analogues to trace diffusion in wood cell walls.

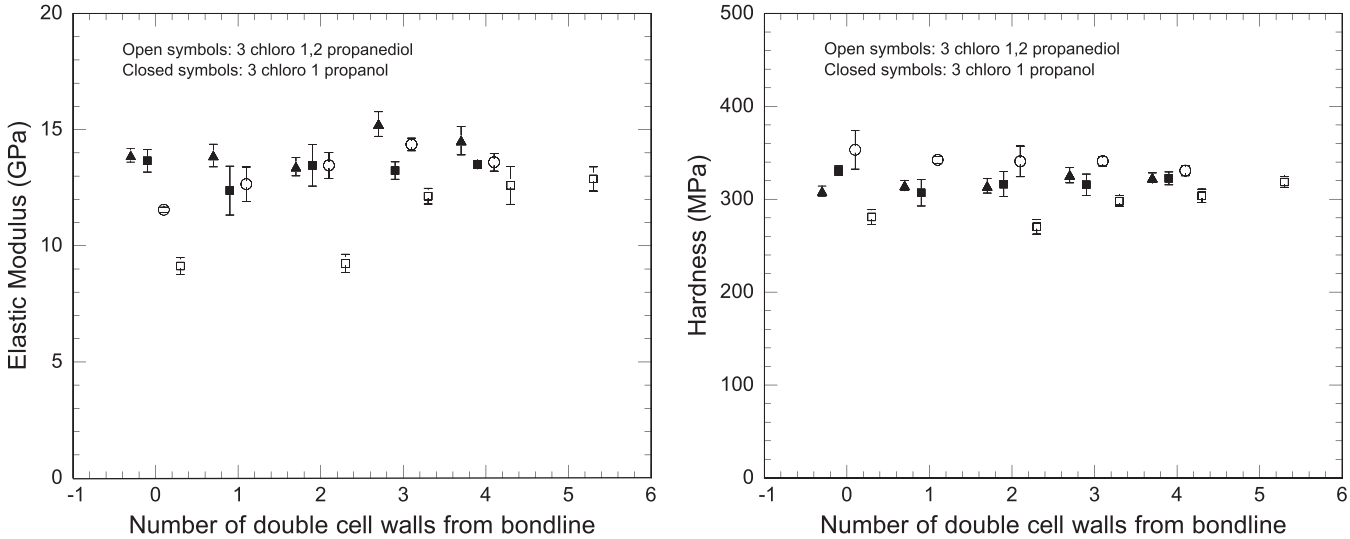

Figure 3.—Average elastic modulus (left) and hardness (right) of S2 cell wall lamina near the wood adhesive bondline. Each datum represents the average of three to eight total nanoindents placed on the S2 cell wall laminae of the double cell wall. The number 0 corresponds to the double cell wall in contact with the adhesive bondline. Each symbol represents data from a different row of cells. Error bars are the estimated standard error of the mean calculated as the standard deviation divided by the square root of the number of nanoindents. Data are slightly shifted on the x *axis for clarity.*

results from the spot aimed at the center of the double cell wall might not be fully representative of the S2 cell wall lamina where the nanoindents were placed, the trends are interesting and provide motivation for future work. A striking feature is the apparently higher quantity of diol in cells adjacent to the bondline compared with the mono-ol glycerin analog. The higher concentration, as well as the higher hydrogen bonding capacity of the diol, is consistent with the larger effect on cell wall elastic modulus relative to the mono-ol shown in Figure 3. The trends in diol concentration and elastic modulus with respect to number of double cell walls from the bondline are also similar. We hypothesize that the difference in analog concentration in wood might be because of differential affinity for the soy and wood, but as yet, the data collected do not allow us to compare diol concentrations (as chlorine) in the adhesive phase to test this hypothesis.

The large potassium (K^+) signal may be unexpected, but dry soy flour contains approximately 2.9 percent K^+ (A. Allen, Ashland Water Technologies, unpublished data, 2013). The clear gradient for ion migration from the adhesive suggests that other ions of interest in various waterborne adhesives such as Na^+, OH^-, and H_3O^+ are likely also moving from adhesives to the wood, changing the pH and ionic content of the adhesive, most probably before cure is complete. Just as a polar size exclusion chromatography column removes small polar molecules from the mobile phase, wood is removing small polar material from the adhesive phase.

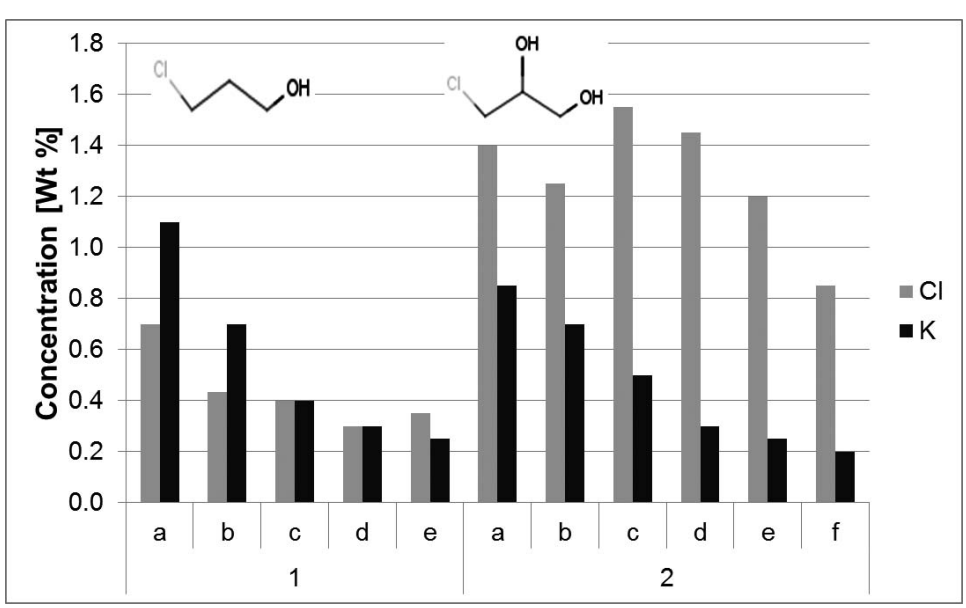

Figure 4.—Concentration of Cl^- and K^+ in sequential daughter cell walls at the bondline (a) and progressing outward.

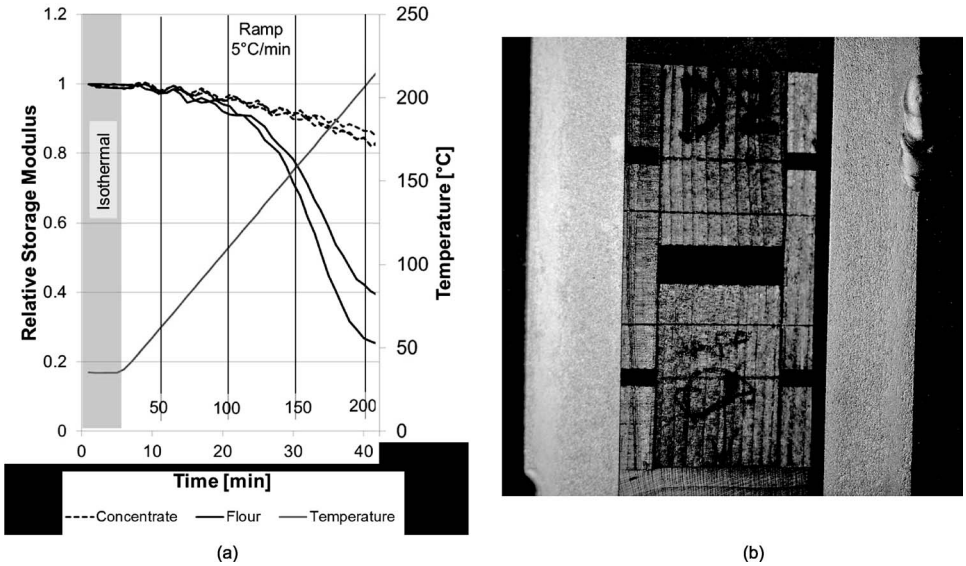

*Figure 5.—Stiffness versus temperature plot for soy flour–polyamidoamine epichlorohydrin (PAE) adhesive on glass cloth in dynamic mechanical analyser (left) showing a dramatic loss in stiffness at 180°C (two replicates shown, solid lines). Soy concentrate (dashed lines) has low-molecular-weight sugars and peptides removed by ethanol extraction and has much better performance at elevated temperature. Soy flour–PAE adhesive on lodgepole pine (*Pinus contorta*; right) held 3 or more hours at 180°C under 2.1-MPa load (O'Dell et al. 2013).*

Heat resistance testing also supports the movement of LMW materials out of soy adhesives into the wood cell walls (O'Dell et al. 2013). Figure 5 (left) contains DMA measurements of soy flour–PAE adhesive (no glycerin) on fiberglass filter paper. The neat adhesive lost ~50 to 60 percent of its initial stiffness at a temperature of 180°C, despite soy flour losing less than 0.5 percent of its original weight at that temperature in thermogravimetric analysis (TGA) experiments. This result would suggest that a soy-PAE bondline would fail the CSA 0112.9 creep test (Canadian Standards Association 2010), where the glued specimen in Figure 5 (right) must hold a 2.1-MPa load for 2 hours at 180°C. Yet all four specimens held 3 or more hours. In this case, we hypothesize that the small (up to a degree of polymerization 3) polysaccharides in soy flour, rather than glycerin, have migrated into the wood. At about 10 percent of the mass of soy flour (Liu 1999), these polysaccharides could have significant impact on thermal softening behavior of the soy proteins. In a similar system, 10 percent sorbitol (MW 182) added to the protein wheat gluten reduced the glass transition temperature by 22°C (Pouplin et al. 1999). Subsequent DMA tests on soy concentrate (soy flour extracted with ethanol to remove small carbohydrates and peptides, as well as denature the protein) show much better thermal softening performance (Fig. 5, left), consistent with our hypothesis. This appears to be another example of wood acting as a polar size exclusion media, removing polar LMW components from the adhesive.

Conclusions

We have shown that glycerin analogs migrate from a soy adhesive into the wood cells adjacent to the bondline, and that cells adjacent to the adhesive containing 3 chloro-1,2 propanediol had lower elastic modulus than control cells. This supports the concept that wood acts as a polar-size exclusion chromatography medium, removing LMW components from the liquid adhesive around it. As a consequence, adhesives cured neat can be chemically, morphologically, and mechanically different from adhesives cured in contact with wood. While this in one sense is well known in the wood adhesives community, it is often forgotten or overlooked in relation to adhesive performance. From a practical standpoint, we recommend that researchers investigating bondline adhesive properties, especially of protein- or polyurethane-based adhesives, consider using adhesive cured in wood contact rather than the common substitute, neat adhesive. We also point out that considering infiltration is useful when attempting to understand wood adhesive behaviors. One way to elevate the level of awareness would be to use the specific terms flow and infiltration when one or the other of these is under discussion, rather than using the general term penetration.

Acknowledgments

We would like to thank Tom Kuster of the Forest Products Laboratory for the SEM-EDS work, as well as Jim Wescott and Tony Allen of Ashland Water Technologies for useful discussions on soy adhesives and soy flour compositional data.

Literature Cited

Bikerman, J. J. 1967. Causes of poor adhesion: Weak boundary layers. *Indust. Eng. Chem.* 59(9):40–44.

Canadian Standards Association (CSA). 2010. Evaluation of adhesives for structural wood products (exterior exposure). CSA 0112.9. Canadian Standards Association, Toronto.

Frazier, C. 2013. Structure property relationships of polyurethane adhesives. Presented at the International Conference on Wood Adhesives, October 9–11, 2013, Toronto.

Frihart, C. R. 2006. Wood structure and adhesive strength. *In:* Characterization of the Cellulosic Cell Wall. D. D. Stokke and L. H. Groom (Eds.). Blackwell, Ames, Iowa.

Frihart, C. R. 2009. Adhesive groups and how they relate to the durability of bonded wood *J. Adhes. Sci. Technol.* 23:601–617.

Gindl, W. and H. S. Gupta. 2002. Cell wall hardness and Young's

modulus of melamine-modified spruce wood by nano-indentation. *Compos. Part A* 33:1141–1145.

Gindl, W., T. Schoberl, and G. Jeronimidis. 2004a. The interphase in phenol-formaldehyde and polymeric methylene diphenyl-di-isocyanate glue lines in wood. *Int. J. Adhes. Adhes*. 24:279–286.

Gindl, W., T. Schoberl, and G. Jeronimidis. 2004b. Corrigendum. *Int. J. Adhes. Adhes*. 24:535.

Grigsby, W. and A. Thumm. 2010. Visualization of biomaterials on wood fiber. *In:* International Conference on Wood Adhesives 2009, September 28–30, 2009, South Lake Tahoe, Nevada; Forest Products Society, Madison, Wisconsin.

Grigsby, W. and A. Thumm. 2012. The interactions between wax and UF resin in medium density fibreboard. *Eur. J. Wood Wood Prod*. 70(4):507–517.

Grigsby, W. J., J. E. P. Carpenter, A. Thumm, R. Sargent, and N. Hati. 2015. Labile extractable urea-formaldehyde resin components from medium-density fiberboard. *Forest Prod. J*. 65(1–2):15–19.

Hansen, C. (Ed.). 2000. Hansen's Solubility Parameters: A Users Handbook. 2nd ed. CRC Press, Taylor and Francis Group, Boca Raton, Florida.

Hansen, C. and A. Bjorkman. 1998. The ultrastructure of wood from a solubility parameter point of view. *Holszforschung* 52:335–344.

Hunt, C. G., J. E. Jakes, and W. Grigsby. 2010. Evaluation of adhesive penetration of wood fibre by nanoindentation and microscopy. *In:* Biocomp 2010: 10th Pacific Rim Bio-Based Composites Symposium, October 5–8, 2010, Banff, Alberta, Canada. pp. 216–226.

Jakes, J. E., C. R. Frihart, J. F. Beecher, R. J. Moon, P. J. Resto, Z. H. Melgarejo, and O. M. Surez. 2009. Nanoindentation near the edge. *J. Mater. Res*. 24(3):1016–1031.

Jakes, J. E., C. R. Frihart, J. F. Beecher, R. J. Moon, and D. S. Stone. 2008. Experimental method to account for structural compliance in nanoindentation measurements. *J. Mater. Res*. 23(4):1113–1127.

Kamke, F. A. and J. N. Lee 2007. Adhesive penetration in wood—A review. *Wood Fiber Sci*. 39(2):205–220.

Konnerth, J. and W. Gindl. 2006. Mechanical characterisation of wood-adhesive interphase cell walls by nanoindentation. *Holzforschung* 60(4):429–433.

Konnerth, J., D. Harper, S. H. Lee, T. G. Rials, and W. Gindl. 2008. Adhesive penetration of wood cell walls investigated by scanning thermal microscopy (SThM). *Holzforschung* 62(1):91–98.

Konnerth, J., A. Jaeger, J. Eberhardsteiner, U. Mueller, and W. Gindl. 2006. Elastic properties of adhesive polymers. II. Polymer films and bond lines by means of nanoindentation. *J. Appl. Polym. Sci*. 102(2):1234–1239.

Konnerth, J., A. Valla, and W. Gindl. 2007. Nanoindentation mapping of a wood-adhesive bond. *Appl. Phys. A Mater. Sci. Process*. 88(2):371–375.

Liang, K., G. B. Du, O. Hosseinaei, S. Q. Wang, and H. Wang. 2011. Mechanical properties of secondary wall and compound corner middle lamella near the phenol-formaldehyde (PF) adhesive bond line measured by nanoindentation. *Adv. Mater. Res*. 236–238:1746–1751.

Liu, K. 1999. Soybeans Chemistry, Technology, and Utilization. Aspen Publications, Gaithersburg, Maryland.

Mantanis, G. I., R. A. Young, and R. M. Rowell. 1994. Swelling of wood, Part II. Swelling in organic liquids. *Holzforschung* 48:480–490.

Obataya, E. and J. Gril. 2005. Swelling of acetylated wood. I. Swelling in organic liquids. *J. Wood Sci*. 51:124–129.

O'Dell, J. L., C. G. Hunt, and C. R. Frihart. 2013. High temperature performance of soy-based adhesives. *J. Adhes. Sci. Technol*. 27:2027–2042.

Oliver, W. C. and G. M. Pharr. 1992. An improved technique for determining hardness and elastic-modulus using load and displacement sensing indentation experiments. *J. Mater. Res*. 7(6):1564–1583.

Pouplin, M., A. Redl, and N. Gontard. 1999. Glass transition of wheat gluten plasticized with water, glycerol, or sorbitol. *J. Agric. Food Chem*. 47(2):538–543.

Stöckel, F., J. Konnerth, J. Moser, W. Kantner, and W. Gindl-Altmutter. 2012. Micromechanical properties of the interphase in pMDI and UF bond lines. *Wood Sci. Technol*. 46(4):611–620.

Stone, D. S., J. E. Jakes, J. Puthoff, and A. A. Elmustafa. 2010. Analysis of indentation creep. *J Mater. Res*. 25(4): 611–621.

Tarkow, H., W. C. Feist, and C. F. Southerland. 1965. Interpenetration of wood and polymeric materials, II: Penetration versus molecular size. *Forest Prod. J*. 16(10):61–65.

Wimmer, R., B. Lucas, T. Tsui, and W. Oliver. 1997. Longitudinal hardness and Young's modulus of spruce tracheid secondary walls using nanoindentation technique. *Wood Sci. Technol*. 31(2):131–141.

Yan, L., J. Cao, W. Gao, X. Zhou, and G. Zhao. 2011. Interaction between glycerin and wood at various temperatures from stress relaxation approach. *Wood Sci. Technol*. 45(2):215–222.